

1 **Title: Motor skill learning decreases movement variability and increases planning**

2 **horizon**

3

4 **Authors**

5 Luke Bashford^{1,2,3,4,*}, Dmitry Kobak^{1,2,3,5,6,*}, Jörn Diedrichsen⁷, Carsten Mehring^{1,2,3}

6

7 ¹Bernstein Center Freiburg, University of Freiburg, Freiburg, Germany

8 ²Faculty of Biology, University of Freiburg, Freiburg, Germany

9 ³Imperial College London, London, UK

10 ⁴California Institute of Technology, Pasadena, CA, USA

11 ⁵Champalimaud Centre for the Unknown, Lisbon, Portugal

12 ⁶Institute for Ophthalmic Research, Tübingen University, Tübingen, Germany

13 ⁷Brain and Mind Institute & Department for Computer Science, University of Western

14 Ontario, Ontario, Canada

15 *Equal contribution

16

17 **Corresponding author**

18 Luke Bashford, bashford@caltech.edu

19 **Abstract**

20

21 We investigated motor skill learning using a path tracking task, where human subjects had to
22 track various curved paths at a constant speed while maintaining the cursor within the path
23 width. Subjects' accuracy increased with practice, even when tracking novel untrained paths.
24 Using a "searchlight" paradigm, where only a short segment of the path ahead of the cursor
25 was shown, we found that subjects with a higher tracking skill differed from the novice
26 subjects in two respects. First, they had lower movement variability, in agreement with
27 previous findings. Second, they took a longer section of the future path into account when
28 performing the task, i.e. had a longer planning horizon. We estimate that between one third
29 and one half of the performance increase in the expert group was due to the longer planning
30 horizon. An optimal control model with a fixed horizon (receding horizon control) that
31 increases with tracking skill quantitatively captured the subjects' movement behaviour. These
32 findings demonstrate that human subjects not only increase their motor acuity but also their
33 planning horizon when acquiring a motor skill.

34 **New and Noteworthy**

35

36 We show that when learning a motor skill humans are using information about the
37 environment from an increasingly longer amount of the movement path ahead to improve
38 performance. Crucial features of the behavioural performance can be captured by modeling
39 the behavioural data with a receding horizon optimal control model.

40 **Introduction**

41

42 The human motor system can acquire a remarkable array of motor skills. Informally, a person
43 is said to be “skilled” if he or she can perform faster and at the same time more accurate
44 movements than other, unskilled, individuals. What we don't know, however, is what learning
45 processes and components underlie our ability to move better and faster. One component
46 may be relatively “cognitive”, involving the faster and more appropriate selection and
47 planning of upcoming actions (Diedrichsen and Kornysheva 2015; Wong et al. 2015).
48 Another component may be related to motor execution – the ability to produce and finely
49 control difficult combinations of muscle activations, also called “motor acuity” (Shmuelof et
50 al. 2012; Waters-Metenier et al. 2014). Depending on the structure of the task, changes in
51 visuo-motor processing or feedback control may also contribute to skill development. Motor
52 adaptation extensively studied using visuomotor and force perturbations (Shadmehr et al.
53 2010), may play a certain role in stabilizing performance, but it cannot by itself lead to
54 improvements in the speed-accuracy trade-off (Wolpert et al. 2011).

55

56 A task commonly used in the experiments on motor skill learning is sequential finger tapping,
57 where subjects are asked to repeat a certain tapping sequence as fast and as accurately as
58 possible (Karni et al. 1995, 1998; Petersen et al. 1998; Walker et al. 2002). Improvement in
59 such a task can continue over days, but previous papers have focussed mostly on the learning
60 that is specific to the trained sequence(s) (Karni et al. 1995).

61

62 Many real-world tasks, however, do not involve the production of a fixed sequence of motor
63 commands, but the flexible planning and execution of movements. Such flexibility is often
64 well described by optimal feedback control models (Braun et al. 2009; Diedrichsen et al.

65 2010; Todorov and Jordan 2002) where the skilled actor appears to compute “on the fly” the
66 most appropriate motor command for the task at hand. This requires demanding computations
67 (Todorov and Jordan 2002), and the human motor system likely has found heuristics to deal
68 with this complexity. One way to reduce complexity of the control problem is to not optimize
69 the whole sequence of motor commands that will achieve the ultimate goal, but to only
70 optimise the current motor command for a short distance into the future. This idea is called
71 receding horizon control, also known as model predictive control (Kwon and Han 2005).
72 Under this control regime, the system computes a feedback control policy that is optimal for a
73 finite planning horizon. The control policy is then continuously updated as the movement
74 goes on and the planning horizon is being shifted forward. This allows for adaptability, e.g. it
75 can flexibly react to perturbations or unexpected challenges, as sensory information becomes
76 available. Recent studies provided indirect evidence that favour the optimisation of short
77 time-periods of a motor command (Dimitriou et al. 2013). The notion of planning horizon
78 also arises in reinforcement learning, e.g. in the context of the so-called successor
79 representation (Momennejad et al. 2017).

80

81 Motivated by these ideas, we propose that some of the skill of a down-hill skier or a race-car
82 driver may lie not only in the increased ability to execute difficult motor commands (e.g. due
83 to increased motor acuity), but also in the ability to plan further ahead and to optimize the
84 movements for a longer time period into the future. In addition, we propose that the time span
85 that subjects plan ahead increases with experience, leading to an increasing performance with
86 training.

87

88 To test this idea, we designed an experimental condition which would allow us to measure
89 the planning horizon that skilled actors are using when executing long sequence of

90 movements that need to be planned “on the fly” – i.e. where the actual sequence of
91 movements cannot be memorized. For this, we developed a path tracking task, where subjects
92 had to maintain their cursor within a path that was moving towards them at a fixed speed. A
93 similar task has been previously used in motor control research (Poulton 1974), using a
94 mechanical apparatus with paths drawn on a paper roll that was moving at a fixed speed. It
95 has been shown that subjects are able to increase their accuracy with training, but the
96 different computational strategies between expert subjects and naïve performers remain
97 unclear. In our study we use ‘searchlight’ trials in which subjects see various lengths of the
98 approaching path ahead of their cursor to probe subjects forward planning and compare
99 experts and novices in this respect.

100

101 **Materials and Methods**

102

103 **Subjects**

104 62 experimentally naïve subjects took part in this experiment (33 males and 29 females, age
105 range 20-52 years old). Subjects gave written informed consent and were paid 10 €/h. The
106 experimental procedures received ethics approval from the University of Freiburg.

107

108 **Setup**

109 Subjects sat at a desk looking at a computer monitor (Samsung Syncmaster 226BW) located
110 ~80cm away. A cursor displayed on the screen (Matlab and Psychophysics Toolbox Version
111 3 (Brainard 1997)) was under position control by movements of a computer mouse. The
112 mouse could be moved on the desk in all directions but only the horizontal (left and right)
113 component contributed to the cursor movement: the vertical position of the cursor was fixed
114 at 5.7mm above the base of the screen.

115

116 **Task**

117 To begin each trial subjects had to press the space bar. This displayed the cursor ($R=2.9\text{mm}$,
118 1.1cm from the bottom of the screen) and the path (width = 2.83cm) that extended from the
119 top to bottom of the screen (30cm). The path continuously moved downward on the screen at
120 a vertical speed of 34.1cm/s . The initially visible path was a straight line centered in the
121 middle of the screen with the cursor positioned in the middle of the path. Once this initial
122 section moved through the screen, the path then followed a random curvature (Fig. 1A).
123 Subjects were instructed to keep the cursor between the path borders at all times moving only
124 in the horizontal plane and were told to be as accurate as possible. The cursor and path were

125 displayed in white if the cursor was within the path and both turned red when it was outside
126 the path, always on a black background.

127

128 The cursor position was sampled at 60 Hz and the tracking accuracy was defined for each
129 trial as the percentage of time steps when the cursor was inside the path. Running accuracy
130 values were continuously displayed in the top left corner of the screen and final accuracies
131 were displayed between the trials.

132

133 This experiment is based on a previous version where subjects were asked to track static
134 randomly curved paths in 2D as quickly as possible without touching the sides [unpublished
135 data, (Bashford et al. 2014)]. We later found that the 1D paradigm presented here was better
136 suited to study the planning horizon as the speed was fixed.

137 **Paradigm**

138 Subjects were randomly assigned into two groups: expert (N=32) and naive (N=30). The
139 paradigm included a training (expert group only) and a testing (all subjects) phase. Subjects
140 in the expert group trained over 5 consecutive days, each day completing 30 minutes of path
141 tracking (10 of 3-minute trials with short breaks in-between, searchlight length (s) 100%). If
142 the performance improved from one trial to the next subjects saw a message saying
143 “Congratulations! You got better! Keep it up!”, otherwise the message “You were worse this
144 time! Try to beat your score!” was shown. The training paths were randomly generated on the
145 fly. Experts performed the testing set of trials after a short break following training on the
146 final (5th) day. Naïve subjects performed only the testing set of trials.

147

148 The testing phase lasted 30 min (30 of 1-minute trials with breaks in-between) using 30
149 different pre-generated paths that were the same for all subjects. The testing phase in this

150 experiment contained 3 normal trials ($s=100\%$) and 27 searchlight trials ($s=10-90\%$) where
151 some upper part of the path was not visible. Three blocks of 10 trials with the searchlight
152 length ranging from $s=10\%$ to $s=100\%$ (in steps of 10%) were presented, with the order
153 shuffled in each block; the same fixed pseudorandom sequence was used for all subjects.

154

155 **Path generation**

156 Paths were generated before each trial start during training and a pre-generated fixed set was
157 produced in the same way for testing. Each path was initialized to start at the bottom middle
158 of the screen and the initial 30 cm of each path were following a straight vertical line.
159 Subsequent points of the path midline had a fixed Y step of 40 pixels (1.1 cm) and random
160 independent and identically distributed (iid) X steps drawn from a uniform distribution from
161 1 to 80 pixels (2.7mm – 2.2cm). Any step that would cause the path to go beyond the right or
162 left screen edges was recalculated. The midline was then smoothed with a Savitzky-Golay
163 filter (12th order, window size 41) and used to display path boundaries throughout the trial.
164 All of the above parameters were determined in pilot experiments to create paths which were
165 very hard but not impossible to complete after training.

166

167 **Statistical analysis**

168 In all cases, we used nonparametric rank-based statistical tests to avoid relying on the
169 normality assumption. In particular, we used Spearman's correlation coefficient instead of the
170 Pearson's coefficient, Wilcoxon signed-rank test instead of paired two-sample t-test, and
171 Wilcoxon-Mann-Whitney rank sum test instead of unpaired two-sample t-test.

172

173 We initially recorded N=10 subjects in each group and observed statistically significant
174 ($p<0.05$) effect that we are reporting here: positive correlation between the asymptote
175 performance and the horizon length, as estimated via the changepoint and exponential
176 models. We then recorded another N=20/22 (naïve/expert) subjects per group to confirm this
177 finding. This internal replication confirmed the effect ($p<0.05$). The final analysis reported in
178 this study was based on all N=62 subjects together. A preliminary version of the analysis for
179 the initial N=10/10 subjects can be found in our preprint (Bashford et al. 2014), but note that
180 it used a different way to estimate planning horizon compared to the procedure presented
181 here, and so the values are not directly comparable.

182

183 **Changepoint and Exponential model**

184 We used two alternative models to describe the relationship between the searchlight length
185 and the accuracy: a linear changepoint model and an exponential model. We used two
186 different models to increase the robustness of our analysis and both models support our
187 conclusions.

188

189 The changepoint model is defined by

$$y = \begin{cases} cs + o & \text{if } s \leq h_{cp} \\ ch_{cp} + o & \text{if } s > h_{cp} \end{cases}$$

190 where y is the subject's performance, s the searchlight length and (c, o, h_{cp}) are the subject-
191 specific parameters of the model which define the baseline performance at searchlight 0%
192 (o), the amount of increase of performance with increasing searchlight (c) and the planning
193 horizon (h_{cp}) after which the performance does not increase any further.

194

195 The exponential model is defined by

$$y = \psi - \exp(-\rho s + d)$$

196 where the subject-specific parameters (ψ , d , ρ) specify the performance at searchlight 0%
197 ($\psi - \exp[d]$), the asymptote for large searchlights (ψ) and the speed of performance increase
198 (ρ).

199 This function monotonically increases but it never plateaus. The speed of the increase
200 depends on the parameter ρ with larger values meaning faster approaching the asymptote. We
201 used the following quantity as a proxy for the “effective” planning horizon: $10 + \log(5)/\rho$. It
202 can be understood as the searchlight length that leads to performance being five times closer
203 to the asymptote than at $s=10\%$. The $\log(5)$ factor was chosen to yield horizon values of
204 roughly the same scale as with the changepoint model above.

205

206 Both models (changepoint and exponential) were fit to the raw performance data of each
207 subject, i.e. to the 30 data points, 3 for each of the 10 searchlight length values. The
208 exponential fit (see Equation 2 in the Results) was done with the Matlab's `nlinfit()` function,
209 implementing Levenberg-Marquardt nonlinear least squares algorithm. The changepoint fit
210 (see Equation 1 in the Results) was done with a custom script that worked as follows. It tried
211 all values of h_{cp} on a grid that included $s=10\%$ and then went from $s=20\%$ to $s=100\%$ in 100
212 regular steps. For each value of h_{cp} the other two parameters can be found via linear
213 regression after replacing all $s > h_{cp}$ values with h_{cp} . We then chose h_{cp} that led to the smallest
214 squared error.

215

216 **Trajectory analysis**

217 To shed light on the learning process we analysed additional parameters of the subjects'
218 movement trajectories.

219

220 First, we computed the time lag between the subjects' movement trajectories and the midline
221 of the paths (Fig. 3A-B). To compute the lags, we interpolated both cursor trajectories and
222 path midlines 10-fold (to increase the resolution of our lag estimates) and concatenated all
223 three trials from the same subject and searchlight length. We computed the Pearson
224 correlation coefficient between cursor trajectory and path midline for time shifts from of -300
225 to 300 ms, and defined the time lag as the time shift maximizing the correlation. We then
226 used the obtained lags to compute mean-squared-error between the lagged path midline and
227 the subject's trajectory for each subject and searchlight length (Fig. 3C-D).

228

229 Second, we extracted the cursor trajectories in all sections across all paths that shared a
230 similar curved shape to explore the differences in cursor position at the apex of the curve
231 (Fig. 4). The segments were selected automatically by sliding a window of length 18 cm
232 across the path. We included all segments that were lying entirely to one side (left or right) of
233 the point in the middle of the sliding window ("C-shaped" segments), with the upper part and
234 the lower part both going at least 4.5 cm away in the lateral direction (see Fig. 4). Our results
235 were not sensitive to modifying the exact inclusion criteria.

236

237 To draw the 75% coverage areas of the path inflection points in each group (Fig. 4), we first
238 performed a kernel density estimate of these points using the Matlab function `kde2d()`, which
239 implements an adaptive algorithm suggested in (Botev et al. 2010). After obtaining the 2d
240 probability density function $p(x)$, we found the largest h such that $\int p(x)dx > 0.75$ over the area
241 where $p(x) > h$. We then used Matlab's `contour()` function to draw contour lines of height h in
242 the $p(x)$ function.

243

244 **Receding horizon model**

245 We modeled subjects' behaviour by a stochastic receding horizon model in discrete time t . In
 246 receding horizon control (RHC,(Kwon and Han 2005)) motor commands u_t are computed to
 247 minimize a cost function L_t over a finite time horizon of length h :

$$\text{minimize } L_t(\{x_t\}, \{u_t\}) \#(1)$$

$$\text{subject to } L_t = \sum_{k=1}^h l_{t+k}$$

$$x_{t+1} = f(x_t, u_t)$$

248 where f defines the dynamics of the controlled system. Equation (1) is equivalent to an
 249 optimal control problem over the fixed future interval $[t + 1, t + h]$. Solving (1) yields a
 250 sequence of optimal motor commands $\{u_0^{opt}, u_1^{opt}, \dots, u_{h-1}^{opt}\}$. The control applied at time t is
 251 the first element of this sequence, i.e. $u_t = u_0^{opt}$. Then, the new state of the system x_{t+1} is
 252 measured (or estimated) and the above optimization procedure is repeated, this time over the
 253 future interval $[t + 2, t + 1 + h]$, starting from the state x_{t+1} .

254

255 Applying RHC to our experimental task, the dynamics of the cursor movement was modeled
 256 by a linear first-order difference equation:

$$257 \quad x_{t+1} = x_t + u_{t-\tau} + \eta_t \quad \eta_t \in \mathcal{N}(0, \sigma^2) \#(2)$$

258 where t is the time step, x_t the cursor position at time t , u_t is the motor command applied at
 259 time t and τ the motor delay. η_t is the motor noise which was modeled as additive Gaussian
 260 white noise with zero mean and variance σ^2 . We assumed that the controller minimizes the
 261 following cost function

$$L_t = \sum_{k=\tau+1}^h [-\log(q_{t+k}) + \lambda |u_{t-\tau+k-1}|^2] \#(3)$$

262 where L_t is the expected cost at time t , q_{t+k} is the probability of the cursor being inside the
 263 path at time $t+k$, h is the length of the horizon in time and λ is the weight of the motor
 264 command penalty. At every time step t , L_t is minimized to compute u_t . The cost function in
 265 (3) reflects a trade-off between accuracy (first term, i.e. $\log[q_{t+k}]$) and effort (second term)
 266 whereas their relative importance is controlled by λ . Cost functions with a similar accuracy-
 267 effort trade-off have been used previously to successfully model human motor behaviour
 268 (Braun et al. 2009; Diedrichsen 2007; Todorov and Jordan 2002).

269 We assumed that subjects have acquired a forward model of the control problem including
 270 the variance of the motor noise σ^2 . We also assumed that subjects have an accurate estimate
 271 of the position of the cursor at time t , i.e. x_t is known. Under these assumptions the
 272 probability distribution of the cursor position at future times $t+k$, can be computed by:

$$p(x_{t+k}|x_t, \{u_{t-\tau}, u_{t-\tau+1}, \dots, u_{t-\tau+k-1}\}) = \frac{1}{\sqrt{2\pi k\sigma^2}} e^{-\frac{(\hat{x}_{t+k})^2}{2k\sigma^2}} \#(5)$$

273 with

$$\hat{x}_{t+i} = x_t + \sum_{l=1}^i u_{t-\tau+l-1} \#(6)$$

274 The probability of the cursor being inside the path is then given by

$$q_{t+k} = \int_{m_{t+k}-\frac{w}{2}}^{m_{t+k}+\frac{w}{2}} \frac{1}{\sqrt{2\pi k\sigma^2}} e^{-\frac{(\hat{x}_{t+k}-z)^2}{2k\sigma^2}} dz \#(7)$$

275 where m_t is the position of the midline of the path at time t and w the width of the path. The
 276 receding horizon model assumes that motor commands u_t are computed by minimizing the
 277 cost L_t in each time step t for a fixed and known set of model parameters ($h, \lambda, \tau, \sigma^2$). We
 278 simplify the optimisation problem by approximating q_{t+k} by

$$q_{t+k} \approx w \frac{1}{\sqrt{2\pi k\sigma^2}} e^{-\frac{(\hat{x}_{t+k}-m_{t+k})^2}{2k\sigma^2}} \#(8)$$

279 The higher $k\sigma_k^2$ is relative to the path width w , the higher the accuracy of this approximation.

280 Note that the squared error is scaled by $k\sigma^2$ and hence, errors in the future are discounted.

281 This is a consequence of the model of the cursor dynamics in equation (2).

282 Using equation (8) and removing all terms which do not depend on u_t , we can derive a

283 simplified cost function

$$\tilde{L}_t = \sum_{k=\tau+1}^h \left[\frac{(\hat{x}_{t+k} - m_{t+k})^2}{2k\sigma^2} + \lambda |u_{t-\tau+k-1}|^2 \right] \#(9)$$

284 Equation (9) shows that the trade-off between accuracy and the magnitude of the motor

285 commands is controlled by $\sigma^2\lambda$. We therefore can eliminate one parameter and use the

286 equivalent cost function

$$\tilde{L}_t = \sum_{k=\tau+1}^h \left[\frac{(\hat{x}_{t+k} - m_{t+k})^2}{2k} + \tilde{\lambda} |u_{t-\tau+k-1}|^2 \right] \text{ with } \tilde{\lambda} = \sigma^2\lambda \#(10)$$

287 The gradient of \tilde{L}_t is given by

$$\frac{\partial \tilde{L}_t}{\partial u_{t+j}} = 2\tilde{\lambda} u_{t+j} + \sum_{k=j+(\tau+1)}^h \left[\frac{(\hat{x}_{t+k} - m_{t+k})}{k} \right] \#(11)$$

288 with $j = 0, \dots, h - (\tau + 1)$. The Hessian of \tilde{L}_t is given by

$$\frac{\partial^2 \tilde{L}_t}{\partial u_{t+m} \partial u_{t+n}} = 2\delta_{m,n} \tilde{\lambda} + \sum_{k=\max(m,n)+(\tau+1)}^h \frac{1}{k} \#(12)$$

289 with $m, n = 0, \dots, h - (\tau + 1)$. For $\tilde{\lambda} = 0$ all pivots of the Hessian matrix in (12) are positive

290 and therefore the Hessian is positive definite for $\tilde{\lambda} = 0$. For the general case $\tilde{\lambda} > 0$ the

291 Hessian in (12) remains positive definite as $H_2 = H_1 + D$ is positive definite if H_1 is positive

292 definite and D is a diagonal matrix with only positive diagonal entries. Given the positive

293 definiteness of the Hessian in (12) we can conclude that the cost function \tilde{L}_t is strictly convex

294 with a unique global minimum. Setting the gradient (12) to $\mathbf{0}$ defines a system of $h-\tau$ linear

295 equations with $h-\tau$ unknowns ($u_t, \dots, u_{t+h-(\tau+1)}$) which solution minimizes \tilde{L}_t . The solution
296 can be computed efficiently using standard numerical techniques. We used the ‘linsolve’
297 function of MATLAB which uses LU factorization.

298 When applying the model to the searchlight path we made the additional assumption that the
299 model horizon increases with searchlight length s up to a maximal value h_{max} beyond which
300 the model horizon remains constant:

$$h(s) = \begin{cases} s, & s < h_{max} \\ h_{max}, & s \geq h_{max} \end{cases} \#(14)$$

301 We used the same time step of 1/30s in the model as in the experiment. For a given set of
302 model parameters ($h_{max}, \lambda, \tau, \sigma^2$) we simulated the model 100 times with independent
303 realizations of the motor noise. For each model trajectory we computed the time inside the
304 path and the lag in the same way as they were computed for the subjects’ trajectories. To
305 obtain the time inside the path and the lag for a set of model parameters we averaged the
306 obtained values across the 100 noise realizations.

307 The model was simulated on the searchlight paths to study the influence of the model horizon
308 h_{max} and the motor noise σ^2 on performance and lag. To this end, we first simulated the
309 model for the shortest searchlight paths (10%) assuming that h_{max} is at least as long as the
310 searchlight length at 10% (=3cm) and using a motor delay of $\tau=200$ ms. The model was
311 simulated using 50 logarithmically spaced values between 10^{-3} and 10^{+3} for λ and 45 values
312 for σ^2 composed of 5 linearly spaced values between 0 and 0.04 and 40 linearly spaced
313 values between 0.05 and 2. Together, this results in $45 \times 50 = 2250$ different parameter sets in
314 total. From these sets, we chose values for λ and σ^2 which yielded a similar performance and
315 lag as experimentally observed for the 10% searchlight (i.e. 45% time inside the path and a
316 lag of 200ms). Using these parameter values, the model was then simulated for all searchlight
317 paths for different model horizons. From the resulting performance as a function of

318 searchlight lengths we computed the change-point in the same way as for the experimental
319 data. In addition, the model was also simulated for different values of the motor noise and the
320 change-point of the performance was computed for different noise levels as above. These
321 analyses allowed us to investigate the influence of the model horizon and model motor noise
322 on the change-point of the performance curve (see Fig. 5). To establish the robustness of the
323 model results, we repeated the above simulations and analyses for different values of the
324 motor delay using $\tau=33\text{ms}$, 100ms and 233ms .

325 Parts of the modeling computations were run on the high-performance computing cluster
326 NEMO of the University of Freiburg (<http://nemo.uni-freiburg.de>) using Broadwell E5-
327 2630v4 2.2 GHz CPUs.

328 All analysis code is available at <https://github.com/dkobak/path-tracking>.

329

330 **Results**

331

332 **Learning the Tracking Skill**

333 We designed an experiment where subjects had to track a path moving towards them at a
334 fixed speed (Fig. 1A and Methods). The narrow and wiggly path was moving downwards on
335 a computer screen while the cursor had a fixed vertical position in the bottom of the screen
336 and could only be moved left or right. Accuracy, our performance measure, was defined as
337 the fraction of time that the cursor spent inside the path boundaries. One group of subjects
338 (the expert group, N=32) trained this task for 30 minutes on each of 5 consecutive days.
339 Another group (the naïve group, N=30) did not have any training at all. Both groups then
340 performed a testing block that we describe below.

341

342 Over the course of five training days, the experts' accuracy increased from $66.9 \pm 8.0\%$ to
343 $79.6 \pm 6.4\%$ (mean \pm SD across subjects, first and last training day respectively) as shown on
344 Figs 1B-C, with the difference being easily noticeable and statistically significant ($p=8 \times 10^{-7}$,
345 $z=4.9$, Wilcoxon signed rank test; Cohen's $d=1.8$, N=32). As all paths generated during the
346 training were different, this difference cannot be ascribed to memorizing the path, therefore
347 this improvement represents the genuine acquisition of the skill of path tracking.

348

349 **Searchlight testing**

350 To unravel the mechanisms of skill acquisition we designed testing trials called “searchlight
351 trials”, during which subjects had to track curved paths as usual but could only see a certain
352 part of the path (fixed distance s) ahead of the cursor. The searchlight length s varied between
353 10% and 100% of the whole path length in steps of 10% (the minimal s was ~ 3 cm) to probe

354 subjects' planning horizon. Searchlight testing was conducted after 5 days of training for
355 experts or immediately for novices. During the testing block all subjects completed 30 one-
356 minute-long trials (three repetitions of each of the 10 values of s). The average accuracy at
357 full searchlight $s=100\%$ was $82.8\pm 7.5\%$ for the expert group and $65.7\pm 8.4\%$ for the naïve
358 group (mean \pm SD across subjects), with the difference being highly significant ($p=2\times 10^{-9}$,
359 $z=6.0$, Wilcoxon-Mann-Whitney rank sum test, Cohen's $d=2.2$, $N=62$). The performance of
360 the naïve subjects during 100% searchlight trials ($65.7\pm 8.4\%$) was not significantly different
361 from the initial performance of the expert subjects on their first day of training ($66.9\pm 8.0\%$),
362 where searchlight was also 100% ($p=0.76$, $z=0.3$, Wilcoxon-Mann-Whitney rank sum test,
363 Cohen's $d=0.15$, $N=62$).

364

365 Before we present the rest of the data, let us consider several possible ways in which the
366 accuracy can depend on the searchlight length (Fig. 2A). For each subject, accuracy should
367 be a non-decreasing function of searchlight length. The data presented in Poulton (1974)
368 indicate that this function tends to become flat, i.e. subjects reach a performance plateau, after
369 a certain value of the searchlight length that we will call *planning horizon* (Fig. 2A, top),
370 while we assume all subjects will be constrained to the similar poor performance at the
371 smallest searchlight. For the expert group, this function has to reach a higher point at
372 $s=100\%$, which could be achieved in one of two ways. Firstly, it could do so because the
373 initial rise becomes steeper (Fig. 2A, bottom left), due to increased motor acuity after skill
374 learning (Shmuelof et al. 2012, 2014). Alternatively, the expert group could reach a higher
375 point at $s=100\%$ because the initial rise continues longer. This would suggest an increase in
376 the planning horizon (Fig. 2A, bottom right) over which subjects plan and execute motor
377 commands, described well by a receding horizon control (Kwon and Han 2005). It is likely a
378 combination of both is employed by the human motor system during skill learning.

379

380 Fig. 2B shows subjects' accuracy in the searchlights trials as a function of the searchlight
381 length s . All subjects were strongly handicapped at short searchlights, and at the shortest
382 searchlight the performance of the two groups was similar with experts being only marginally
383 better ($42.5 \pm 2.3\%$ for the expert group, $41.4 \pm 1.8\%$ for the naïve group, $p=0.042$, $z=2.0$
384 Wilcoxon-Mann-Whitney rank sum test; Cohen's $d=0.5$, $N=62$).

385

386 Visual inspection of Fig. 2B suggests that both effects sketched in Fig. 2A contribute to
387 expert performance. (i) the planning horizon for the expert group was longer than for the
388 naïve group; and (ii) the expert group had higher accuracies in the initial part of the
389 performance curve, before the performance plateaus, which could be explained by an
390 increased motor acuity.

391

392 To investigate differences in tracking skill between groups, we estimated the planning
393 horizons of individual subjects. For this we fit each subject's performance (y) with a
394 changepoint linear-constant curve (see Methods), where the location of the changepoint
395 defines the horizon length. The initial slope of the changepoint model was significantly
396 different between the two groups ($3.7 \pm 1.2\%/cm$ in the expert group vs. $3.0 \pm 1.2\%/cm$ in the
397 naïve group, mean \pm SD; medians: $3.6\%/cm$ vs. $2.6\%/cm$, $p=0.008$, $z=2.6$, Wilcoxon-Mann-
398 Whitney rank sum test; Cohen's $d=0.6$, $N=62$). Fig. 2C shows that there was a positive
399 correlation between the initial slope and asymptote accuracy ($R=0.49$, $p=6 \times 10^{-5}$ Spearman
400 correlation, $N=62$).

401

402 At the same time, we found that the novice group had an average horizon length of
403 $11.5 \pm 3.6cm$ (mean \pm SD; median: $12.0cm$) and the expert group a horizon length of

404 14.2±3.5cm (median: 13.2cm), with statistically significant difference ($p=0.007$, $z=2.7$,
405 Wilcoxon-Mann-Whitney rank sum test; Cohen's $d=0.8$, $N=62$). We also found a positive
406 correlation between the horizon length and the asymptotic performance ($R=0.34$, $p=0.006$,
407 Spearman correlation, $N=62$) (Fig. 2D).

408

409 In addition to the changepoint model, we also quantified the “effective” planning horizon
410 using a single exponential to fit the individual subjects' performance data (see Methods). This
411 analysis confirmed our results (Fig. 2E). We again observed a significant difference in the
412 effective horizon length between the two groups ($14.76\pm 4.6\text{cm}$ vs. $11.04\pm 4.7\text{cm}$, means±SD
413 for both groups, medians: 13.6cm and 10.7cm, $p=0.002$, $z=3.0$, Wilcoxon-Mann-Whitney
414 rank sum test; Cohen's $d=0.8$, $N=62$). Again, we found a positive correlation between the
415 asymptote performance and the effective horizon length ($R=0.43$, $p=0.0008$, Spearman
416 correlation, $N=62$).

417

418 We therefore conclude that the difference between expert and naïve performances is a
419 combination of both possibilities presented in Fig. 2A. Using the expert and naïve median
420 estimates of the intercept, the slope, and the horizon in the changepoint model, we can
421 estimate the contribution of both effects on the asymptote performance. The changepoint
422 model asymptote performance for the naïve group was 63.5%, compared to 78.7% for the
423 expert group. The model performance of the expert group at the naïve horizon was 74.2%.
424 Hence, approximately 71% of the expert performance gain of 15.2%, was due to the increase
425 in the initial slope (possibly due to increased motor acuity), and the remaining 29% can be
426 attributed to the increase in planning horizon. The identical procedure with mean model
427 parameter estimates instead of median estimates, yields 44% attributable to motor acuity and

428 56% attributable to planning horizon. However, these results do not elucidate whether these
429 processes are causally related (see Discussion).

430

431 **Trajectory analysis**

432 Naïve subjects performed worse than the expert subjects at long searchlights but all subjects
433 performed almost equally badly at short searchlights. What kinematic features can these
434 differences be attributed to?

435

436 Clearly, at short searchlights, performance has to be reactive. To measure how quickly
437 changes in the path were reflected in the motor commands, we computed the time lag
438 between cursor trajectory and path midline (the lag maximizing cross-correlation between
439 them). This analysis was done by pooling all trials for each subject and searchlight length
440 together (see Methods). As Fig. 3A shows, the lag was ~200 ms at $s=10\%$ for all subjects and
441 dropped to ~0 ms at $s=50\%$ for the expert group. While many naïve subjects also decreased
442 their lags to zero, 10 out of 30 never achieved the 0 ms lag. The five naïve subjects showing
443 the largest lags at large searchlights were also those with the worst performance (Fig. 3B).
444 Therefore, there was a strong negative correlation between the asymptote lag (mean across
445 $s=80-100\%$) and the asymptote performance (mean across $s=80-100\%$) of $R=-0.58$ (Fig. 3B,
446 $p=8 \times 10^{-7}$ Spearman correlation, $N=62$).

447

448 We used the obtained lags to compute the root-mean-squared-error (RMSE) between the
449 cursor trajectory and the lagged midline. The obtained RMSE was consistently lower in the
450 expert group than in the naïve group, with difference increasing with searchlight length (Fig.
451 3C). The asymptote RMSE was 1.67 ± 0.31 cm (mean \pm SD across subjects; median: 1.69) in the
452 naïve group and 1.23 ± 0.30 cm (median: 1.13) in the expert group ($p=2.14 \times 10^{-6}$, $z=4.74$,

453 Wilcoxon-Mann-Whitney rank sum test; Cohen's $d=1.44$, $N=62$), and was negatively
454 correlated with the asymptote performance (Fig. 3D; $R=-0.79$, $p=0$, Spearman correlation,
455 $N=62$). This shows that the naive subjects were not simply lagging behind the optimal
456 trajectory, but did larger errors even after accounting for the lag.

457

458 Next, for each testing path we found all segments exhibiting sharp leftward or rightward
459 bends (see materials and methods, our inclusion criteria yielded 13 ± 5 segments per path,
460 mean \pm SD). For each searchlight length and for each subject, we computed the average cursor
461 trajectory over all segments ($N=38\pm 8$ segments per searchlight) after aligning all segments on
462 the bend position (Fig. 4, leftward bends were flipped to align them with the rightward
463 bends). At $s=10\%$ all subjects from both groups follow very similar lagged trajectories,
464 resulting in low accuracy. As searchlight increases, expert subjects reach zero lag and choose
465 more and more similar trajectories, whereas naïve subjects demonstrate a wide variety of
466 trajectories with some of them failing to reach zero lag and others failing to keep the average
467 trajectory inside the path boundaries. To visualize this, we plotted the kernel density estimate
468 75% coverage contour of inflection points for each group. As the searchlight increases, the
469 groups become less overlapping and the naïve group appears to form a bimodal distribution
470 (Fig. 4).

471

472 To study the changes in movement variability produced by subjects after skill learning, we
473 additionally looked at the within-subject variability during the segments defined above at
474 100% searchlight and compared this across groups. To measure the variability in subject's
475 movement on a single subject level, we summed the standard deviations in both x and y
476 directions across inflection points of each single segment. The subjects' averages of these
477 positions are shown in Fig. 4. The summed standard deviations were significantly lower for

478 the expert group (median summed SD=24.1) than for the naïve group (median summed
479 SD=37.6) ($p=1.5 \times 10^{-7}$, $z=-5.2$, Wilcoxon-Mann-Whitney rank sum test, Cohen's $d=1.7$,
480 $N=62$). This effect was not present at 10% searchlight (expert median summed SD=53.3,
481 naïve median summed=49.9, $p=0.94$, $z=0.08$, Wilcoxon-Mann-Whitney rank sum test,
482 Cohen's $d=0.03$, $N=62$).

483

484 In summary, at very short searchlights all subjects performed poorly because in this reactive
485 regime their trajectories lagged behind the path. At longer searchlights the expert subjects
486 were able to plan their movement to accommodate the bends (the longer the searchlight the
487 better), but naïve subjects failed to do so in various respects: either still lagging behind, not
488 being able to execute the fine movements due to lower motor acuity and higher movement
489 variability, or not being able to plan a good trajectory.

490

491 **Receding horizon model analysis**

492 Next, we modeled subjects' behaviour by receding horizon control (RHC). Previously,
493 optimal feedback control models have been proposed as mechanisms by which the human
494 brain computes motor commands. Here we intend to expand this framework to include
495 receding horizon control, a version of optimal feedback control with finite horizons, as a
496 mechanism by which motor commands are computed by the human brain. We illustrate this
497 here by showing that such an approach is able to capture some crucial features of the
498 behavioural results from our experiments.

499

500 In RHC, a sequence of motor commands is computed to minimize the expected cost over a
501 future time interval of finite length, i.e. the horizon. After the first motor command is applied,
502 the optimization procedure is repeated using a time interval shifted one time step ahead. See

503 Methods section for a more detailed and formal description of RHC. As cost function, we
504 used the weighted sum of a measure of inaccuracy (i.e. probability of being outside the path)
505 and the magnitude of the motor cost (see Methods for details). Cost functions with a similar
506 trade-off between movement accuracy and motor command magnitude have been used
507 previously to describe human motor behaviour in different tasks (Braun et al. 2009;
508 Diedrichsen 2007; Todorov and Jordan 2002). The model has four different parameters:
509 horizon (h_{max}), motor noise (σ^2), motor delay (τ) and motor command penalty weight (λ).

510

511 We ran the model on the experimental paths to obtain simulated movement trajectories from
512 which task performance and lag could be computed in the same way as for the experimental
513 trajectories (Fig. 2 and 3). To determine the model parameters λ and σ^2 , we simulated the
514 model for the shortest searchlight paths (10%) using different values of λ and σ^2 while
515 fixing τ at 200ms and assuming that the horizon covers at least the length of the 10%
516 searchlight (Fig. 5A-C). From this parameter scan, we determined the values of λ (0.776) and
517 σ^2 (0.271) for which the model yielded approximately the experimentally observed task
518 performance and lag of 45% and 200ms for the 10% searchlight paths (cf. Fig. 2 and 3).

519

520 Using these parameter values we then simulated the model for all searchlight paths for
521 varying values of the horizon (Fig. 5D, E). As a sanity check, we also simulated the model
522 for varying values of the motor noise with a fixed value of the horizon $h_{max}=14.8\text{cm}$ (Fig.
523 5G, H). Our simulations revealed that both, a larger model horizon as well as a smaller motor
524 noise parameter increased the task performance and decreased the lag for large searchlight
525 lengths. Hence, the experimentally observed higher performances and smaller lags of expert
526 subjects compared to naive (Fig. 2B and 3A) could be explained either by an increased model
527 horizon or by reduced motor noise in the model. However, the searchlight length at which the

528 task performance of the model reached a plateau increased with model horizon while it
529 remained constant or decreased with a smaller motor noise parameter (Fig. 5F, I).
530 Experimentally, on the other hand, we observed that subjects with a higher task performance
531 reached their performance plateau at higher searchlights (Fig. 2D, E). This correlation
532 between performance and plateau onset, that was observed experimentally, cannot be
533 explained by the variation of the motor noise parameter across subjects, but is only consistent
534 with an increase of the model horizon parameter for subjects with higher performance.
535 Moreover, with changing motor noise, the model predicted substantial changes in task
536 performance and lag not only for large but also for short searchlight lengths while
537 experimentally the differences between expert and naïve subjects were small for the 10%
538 searchlight length. Model predictions for changes in planning horizon were again consistent
539 with this experimental observation.

540

541 The analyses of Fig. 5G-I were repeated for various model horizons between 3.4cm and
542 29.6cm (not shown) showing similar patterns as presented in Fig. 5G-I for $h_{max} > 3.4\text{cm}$: the
543 performance change-point tended to remain constant or increase with increasing motor noise;
544 changing motor noise induced a clear change of performance and lag also at short
545 searchlights. For $h_{max}=3.4\text{cm}$ the performance was essentially constant across searchlights for
546 all values of the noise. Furthermore, we repeated the model simulations for motor delays of
547 $\tau=33\text{ms}$, $\tau=100\text{ms}$ and $\tau=233\text{ms}$ and obtained qualitatively similar results (not shown).

548

549 **Discussion**

550

551 We used a paradigm that allowed us to study skill development when humans had to track an
552 unpredictable spatial path. The skill requires fast reactions to new upcoming bends in the
553 road, but also a substantial “planning ahead” component – i.e. the anticipation and
554 preplanning of movements that have to be made in the near future. We used the accuracy, i.e.
555 the fraction of time the cursor was inside the path boundaries, as the measure of performance.
556 We observed a substantial improvement in accuracy after 5 days of training (Fig. 1B,C). The
557 paths were different on every trial, so the improvement in performance cannot be attributed to
558 a memory for the sequence.

559

560 What changes in the motor system occur through learning that allowed skilled subjects to
561 perform better? One component of this improvement is motor acuity (Shmuelof et al. 2012,
562 2014) and corresponds to the subjects’ ability to execute motor commands more accurately.
563 We hypothesized that an additional component is an increased ability to take into account
564 approaching path bends and to prepare for an upcoming movement segment. We directly
565 estimated both effects by using a searchlight testing where only a part of the approaching
566 curve was visible. In agreement with our hypothesis, we found that subjects with a higher
567 tracking skill demonstrated larger planning horizons: on average ~14cm for the expert group
568 vs. ~11cm for the naïve group, corresponding to the time horizons of ~0.4s and ~0.3s
569 respectively. Our results suggest that the increase in planning horizon is not an
570 epiphenomenon but is causally related to the performance increase, as expert subjects showed
571 worse performance when the searchlight was reduced below their planning horizon (Fig. 2C).
572 We estimate that between one third and one half of the performance increase in the expert
573 group was due to the longer planning horizon.

574

575 The improvement of acuity and the extension of planning horizon are not necessarily
576 independent processes and may influence each other. For example, it is possible that
577 improved acuity frees up cognitive resources that allow the expansion of planning horizon.
578 Future work should investigate the causal relationship between these two aspects of skill
579 learning.

580

581 Note that “planning”/“preparing” the movement can be interpreted differently depending on
582 the computational approach. In the framework of optimal control (Todorov and Jordan 2002),
583 subjects do not plan the actual trajectory to be followed, but instead use an optimal time-
584 dependent feedback policy and then execute the movement according to this policy. The
585 observed increase in planning horizon can be interpreted in the framework of model
586 predictive control, also known as receding horizon control, RHC (Kwon and Han 2005). In
587 RHC, the optimal control policy is computed for a finite and limited planning horizon, which
588 may not capture the whole duration of the trial. This policy is then applied for the next
589 control step, which is typically very short, and the planning horizon is then shifted one step
590 forward to compute a new policy. Hence, RHC does not use a pre-computed policy, optimal
591 for an infinite horizon, but a policy which is only optimal for the current planning horizon.
592 Increasing the length of the planning horizon is therefore likely to increase the accuracy of
593 the control policy. In our experiments this would allow for a larger fraction of time spent
594 within the path boundaries. We designed a simple RHC model to test directly which
595 components in the model would have to change through training to quantitatively explain the
596 subject’s behaviour. The dynamics of movement and the cost function were modeled in line
597 with previous studies that used optimal control to describe human behaviour in various motor
598 control and learning tasks (Braun et al. 2009; Diedrichsen 2007; Todorov and Jordan 2002).

599 We ran our RHC model on the experimental paths and demonstrated that it yields
600 qualitatively correct predictions: larger value of model horizons led to performance similar to
601 that of the experts' subjects. Our findings, thus, demonstrate that subjects' behaviour can be
602 understood in the context of RHC, and longer planning horizons of the expert group indicate
603 that subjects learn how to take advantage of future path information to improve motor
604 performance.

605

606 Despite a clear difference in the distribution of planning horizons between the naive and the
607 expert groups (Fig. 2D), there was a substantial overlap: the planning horizon of many naive
608 and expert subjects were similar. While this might simply reflect a moderate effect size
609 combined with inter-subject variability and measurement noise, it also remains a possibility
610 that the difference between groups was largely caused by those naive subjects with very low
611 horizons and expert subjects with very high horizons.

612

613 **Related work**

614 Ideas like the RHC were put forward in a recent study (Ramkumar et al. 2016) that suggested
615 that movements are broken up in 'chunks' in order to deal with the computational complexity
616 of planning over long horizons. That study suggests that monkeys increase the length of their
617 movement chunks during extended motor learning over the course of many days which may
618 be explained by monkeys increasing their planning horizon with learning. At the same time,
619 the efficiency of movement control within the chunks improved with learning which may
620 also be the result of a longer horizon. Despite these potential consistencies with our approach
621 we note that in their model Ramkumar et al. (2016) assumed that 'chunks' are separated by
622 halting points (i.e. points of zero speed) and movements within 'chunks' are optimized

623 independently from each other. Our RHC model does not have independent movement
624 elements but movements are optimized continuously.

625

626 Even though our study, to the best of our knowledge, is the first to directly investigate the
627 evolution of the planning horizon during continuous path tracking, an increase in the planning
628 horizon after learning has been recently demonstrated when learning sequences of finger
629 movements (Ariani et al. 2020). Similar path tracking tasks have been used before (Poulton
630 1974). Using a track that was drawn on a rotating paper roll, these early studies found that the
631 accuracy of the tracking increased with practice and with increasing searchlight length (which
632 was modified by physically occluding part of the paper roll, (Poulton 1974), p 187). These
633 studies, however, did not investigate the effect of learning on the planning horizon.

634

635 More recent studies used path tracking tasks where the goal was to move as fast as possible
636 while maintaining the accuracy (instead of moving at a fixed speed). In all of these studies
637 the identical path was repeatedly presented. In one study subjects had to track a fixed maze
638 without visual feedback and learnt to do it faster as the experiment progressed (Petersen et al.
639 1998); there the subjects had to once “discover” and then remember the correct way through
640 the maze. In another series of experiments, Shmuelof et al. asked subjects to track two fixed
641 semi-circular paths. Subjects became faster and more accurate over the course of several days
642 (Shmuelof et al. 2012), but this increase in the speed and accuracy did not generalize to
643 untrained paths (Shmuelof et al. 2014). In contrast to these previous path tracking studies, we
644 used randomly generated paths throughout the experiment. By investigating the
645 generalization of the path tracking skill to novel paths we could reveal an increasing planning
646 horizon with learning.

647

648 The planning horizon could possibly be inferred from the distance the subject gazes ahead of
649 the cursor, and the inclusion of eye movement data could provide an interesting extension for
650 future work. However, eye movement recordings often do not provide a clear answer in these
651 types of experiments (Green and Bavelier 2006; Lehtonen et al. 2014; Wilkie et al. 2008) and
652 the searchlight paradigm remains the most direct avenue of establishing how much
653 information is used to guide behaviour.

654

655 **Conclusion**

656 In conclusion, we have established that people are able to learn the skill of path tracking and
657 improve their skill over 5 days of training. This increase in motor skill is associated with the
658 increased motor acuity and increased planning horizon. The dynamics of preplanning can be
659 well described by a receding horizon control model.

660 **Acknowledgements**

661 The study was in parts supported by the German Federal Ministry of Education and Research
662 (BMBF) grant 01GQ0830 to BFNT Freiburg-Tübingen. The authors acknowledge support by
663 the state of Baden-Württemberg through bwHPC and the German Research Foundation
664 (DFG) through grant no INST 39/963-1 FUGG. The authors also thank the ‘Struktur- und
665 Innovationsfonds Baden-Württemberg (SI-BW)’ of the state of Baden-Württemberg for
666 funding.

667

668 **Author Contribution**

669 Conceptualization, LB. DK. and CM; Methodology, LB. DK. JD and CM; Formal Analysis,
670 LB. DK and CM; Writing – Original Draft, LB. DK and CM; Writing – Review and Editing,
671 LB, DK, JD and CM.

672

673 **Figure Legends**

674

675 *Figure 1. Experimental Paradigm. (A) Subjects had to track a curved path that was dropping*
676 *down from top to bottom of the screen with a fixed speed of 34 cm/sec by moving the cursor*
677 *horizontally. (B) Expert subjects' performance over the 5 days of training. Bold line shows*
678 *the group average, thin lines show individual subjects (each point is a mean over 3 trials with*
679 *the same searchlight length, 100%). (C) Expert subjects' performance over the 5 days of*
680 *training with the performance on the first day subtracted.*

681

682 *Figure 2. Searchlight testing. (A) Expert subjects were trained to have a higher performance*
683 *at full searchlight length (top). This could be achieved by an increased initial slope (bottom*
684 *left) at smaller searchlight length and/or an increased planning horizon as indicated with*
685 *dashed vertical lines (bottom right). (B) Mean tracking performance for each searchlight*
686 *length for each individual subject, in blue for the expert group and in red for the naïve group.*
687 *Faint lines show individual subjects and bold lines show group means. (C) Relationship*
688 *between the asymptote performance and the initial slope in in the changepoint linear-*
689 *constant model (***: $p < 0.001$). (D-E) Planning horizon for each subject was defined by*
690 *fitting a changepoint linear-constant curve (D) or an exponential curve (E) (see text). Both*
691 *models yield an asymptote performance for each subject; the changepoint model yields a*
692 *horizon length and the exponential fit yields an “effective” horizon length. The scatter plots*
693 *with marginal distributions show relation between the asymptote performance (as a proxy for*
694 *subjects' skill) and their planning horizon. Spearman's correlation coefficients are shown on*
695 *the plot (**: $p < 0.01$, ***: $p < 0.001$). Colour of the dot indicates the group.*

696

697 *Figure 3. Analysis of trajectories. (A) Mean time lag between cursor trajectory and path*
698 *midline, for each searchlight length for each individual subject (faint lines) and mean of per-*
699 *subject values (bold lines), in blue for the expert group and in red for the naïve group. (B)*
700 *Asymptote lag and asymptote performance across subjects. Correlation coefficient is shown*
701 *on the plot (***) $p < 0.001$. Colour of the dot indicates the group. (C) and (D) show the same*
702 *for the root mean square error (RMSE) between the cursor trajectory and the path midline.*

703

704 *Figure 4. Average per-subject trajectories in sharp bends (leftward bends were flipped to*
705 *align them with the rightward bends). Each trajectory is averaged across approximately 40*
706 *bends identified in all paths (the number of bends varied across searchlight lengths, see*
707 *Methods section ‘Trajectory analysis’). Colour of the lines indicates the group. Black lines*
708 *show average path contour. Dots show turning points of the trajectory. Contour lines show*
709 *the kernel density estimate 75% coverage areas. Subplots correspond to searchlight lengths*
710 *$s = 10\%$, 20% , 50% , 60% , 90% and 100% .*

711

712 *Figure 5: Task performance (A) and lag (B) for model simulations of the 10% searchlight*
713 *paths as a function of λ and σ^2 assuming $\tau = 200\text{ms}$ and a model horizon of at least the length*
714 *of the 10% searchlight. Note that for high values of λ and σ^2 the lag may not be reliable due*
715 *to small peaks in the cross-correlogram between the movement trajectories predicted by the*
716 *model and the paths (C). The white lines in (A) and (B) show the value of the parameters*
717 *which yielded a task performance and a lag similar to what was experimentally observed*
718 *(Fig.2 and 3). The intersection of the two lines was at $\lambda = 0.77$ and $\sigma^2 = 0.27$. Using these*
719 *parameter values the model was simulated for all searchlight lengths and for various model*
720 *horizons yielding the task performance and lag shown in (D) and (E). The performance*
721 *curves in (D) were analysed using the same change-point analysis as for the experimentally*

722 *obtained performance curves demonstrating an increasing change-point with increasing*
723 *model horizon before flattening out at around 10cm (F) except for very short model horizons*
724 *for which the performance curves were essentially flat and therefore, the change-point could*
725 *not reliably be detected. Using a fixed horizon of $h_{max}=14.8cm$ and $\lambda =0.77$ model*
726 *performance and lag was computed for varying motor noise (G, H) and the change-point of*
727 *the performance was calculated for different values of the motor noise (I).*

728 **References**

- 729 **Ariani G, Kordjazi N, Diedrichsen J.** The planning horizon for movement sequences.
 730 *bioRxiv* 2020.07.15.204529, 2020.
- 731 **Bashford L, Kobak D, Mehring C.** Motor skill learning by increasing the movement
 732 planning horizon [Online]. *ArXiv14106049 Q-Bio* ,
 733 2014<http://arxiv.org/abs/1410.6049> [15 Dec. 2015].
- 734 **Botev ZI, Grotowski JF, Kroese DP.** Kernel density estimation via diffusion. *Ann Stat* 38:
 735 2916–2957, 2010.
- 736 **Brainard DH.** The Psychophysics Toolbox. *Spat Vis* 10: 433–436, 1997.
- 737 **Braun DA, Aertsen A, Wolpert DM, Mehring C.** Learning Optimal Adaptation Strategies
 738 in Unpredictable Motor Tasks. *J Neurosci* 29: 6472–6478, 2009.
- 739 **Diedrichsen J.** Optimal task-dependent changes of bimanual feedback control and
 740 adaptation. *Curr Biol CB* 17: 1675–1679, 2007.
- 741 **Diedrichsen J, Kornysheva K.** Motor skill learning between selection and execution. *Trends*
 742 *Cogn Sci* 19: 227–233, 2015.
- 743 **Diedrichsen J, Shadmehr R, Ivry RB.** The coordination of movement: optimal feedback
 744 control and beyond. *Trends Cogn Sci* 14: 31–39, 2010.
- 745 **Dimitriou M, Wolpert DM, Franklin DW.** The Temporal Evolution of Feedback Gains
 746 Rapidly Update to Task Demands. *J Neurosci* 33: 10898–10909, 2013.
- 747 **Gelman A, Carlin JB, Stern HS, Rubin DB.** *Bayesian Data Analysis, Second Edition.* 2nd
 748 edition. Boca Raton, Fla: Chapman and Hall/CRC, 2003.
- 749 **Green CS, Bavelier D.** Effect of action video games on the spatial distribution of
 750 visuospatial attention. *J Exp Psychol Hum Percept Perform* 32: 1465–1478, 2006.
- 751 **Karni A, Meyer G, Jezzard P, Adams MM, Turner R, Ungerleider LG.** Functional MRI
 752 evidence for adult motor cortex plasticity during motor skill learning. *Nature* 377:
 753 155–8, 1995.
- 754 **Karni A, Meyer G, Rey-Hipolito C, Jezzard P, Adams M, Turner R, Ungerleider L.** The
 755 acquisition of skilled motor performance : Fast and slow experience-driven changes in
 756 primary motor cortex. *Proc Natl Acad Sci U S A* 95: 861–868, 1998.
- 757 **Kwon WH, Han SH.** Receding Horizon Control: Model Predictive Control for State Models
 758 [Online]. Springer-Verlag.//www.springer.com/la/book/9781846280245 [21 Mar.
 759 2018].
- 760 **Lehtonen E, Lappi O, Koirikivi I, Summala H.** Effect of driving experience on
 761 anticipatory look-ahead fixations in real curve driving. *Accid Anal Prev* 70: 195–208,
 762 2014.
- 763 **Momennejad I, Russek EM, Cheong JH, Botvinick MM, Daw ND, Gershman SJ.** The
 764 successor representation in human reinforcement learning. *Nat Hum Behav* 1: 680–
 765 692, 2017.
- 766 **Petersen SE, Mier H van, Fiez JA, Raichle ME.** The effects of practice on the functional
 767 anatomy of task performance. *Proc Natl Acad Sci* 95: 853–860, 1998.
- 768 **Poulton EC.** *Tracking Skill and Manual Control.* Academic Press, Incorporated, New York,
 769 N.Y., 1974.
- 770 **Ramkumar P, Acuna DE, Berniker M, Grafton ST, Turner RS, Kording KP.** Chunking
 771 as the result of an efficiency computation trade-off. *Nat Commun* 7: 12176, 2016.
- 772 **Shadmehr R, Smith MA, Krakauer JW.** Error Correction, Sensory Prediction, and
 773 Adaptation in Motor Control. *Annu Rev Neurosci* 33: 89–108, 2010.

774 **Shmuelof L, Krakauer JW, Mazzoni P.** How is a motor skill learned? Change and
775 invariance at the levels of task success and trajectory control. *J Neurophysiol* 578–
776 594, 2012.

777 **Shmuelof L, Yang J, Caffo B, Mazzoni P, Krakauer JW.** The neural correlates of learned
778 motor acuity. *J Neurophysiol* 112: 971–980, 2014.

779 **Todorov E, Jordan MI.** Optimal feedback control as a theory of motor coordination. *Nat*
780 *Neurosci* 5: 1226–1235, 2002.

781 **Walker MP, Brakefield T, Morgan A, Hobson JA, Stickgold R.** Practice with Sleep
782 Makes Perfect : Sleep-Dependent Motor Skill Learning. *Neuron* 35: 205–211, 2002.

783 **Waters-Metenier S, Husain M, Wiestler T, Diedrichsen J.** Bihemispheric Transcranial
784 Direct Current Stimulation Enhances Effector-Independent Representations of Motor
785 Synergy and Sequence Learning. *J Neurosci* 34: 1037–1050, 2014.

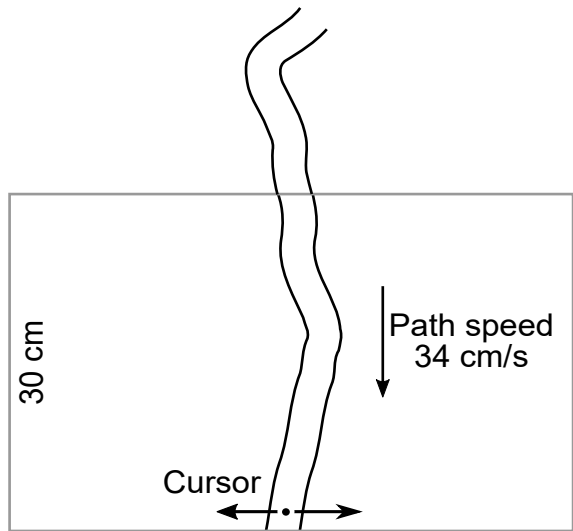
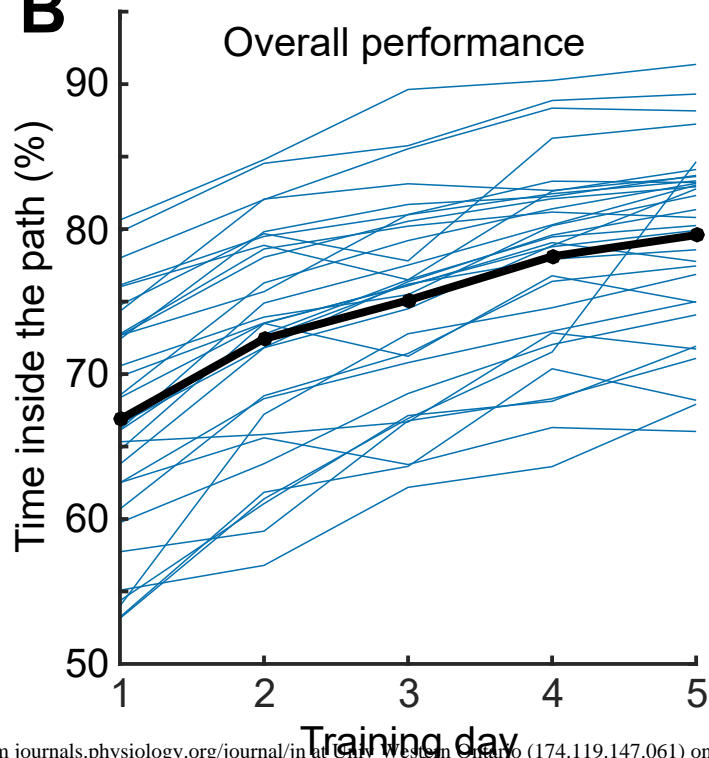
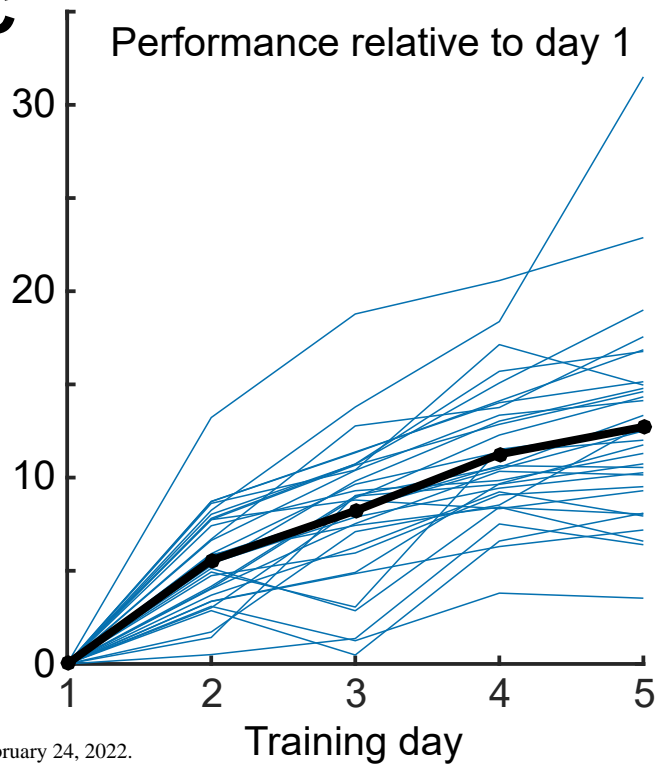
786 **Wilkie RM, Wann JP, Allison RS.** Active gaze, visual look-ahead, and locomotor control. *J*
787 *Exp Psychol Hum Percept Perform* 34: 1150–1164, 2008.

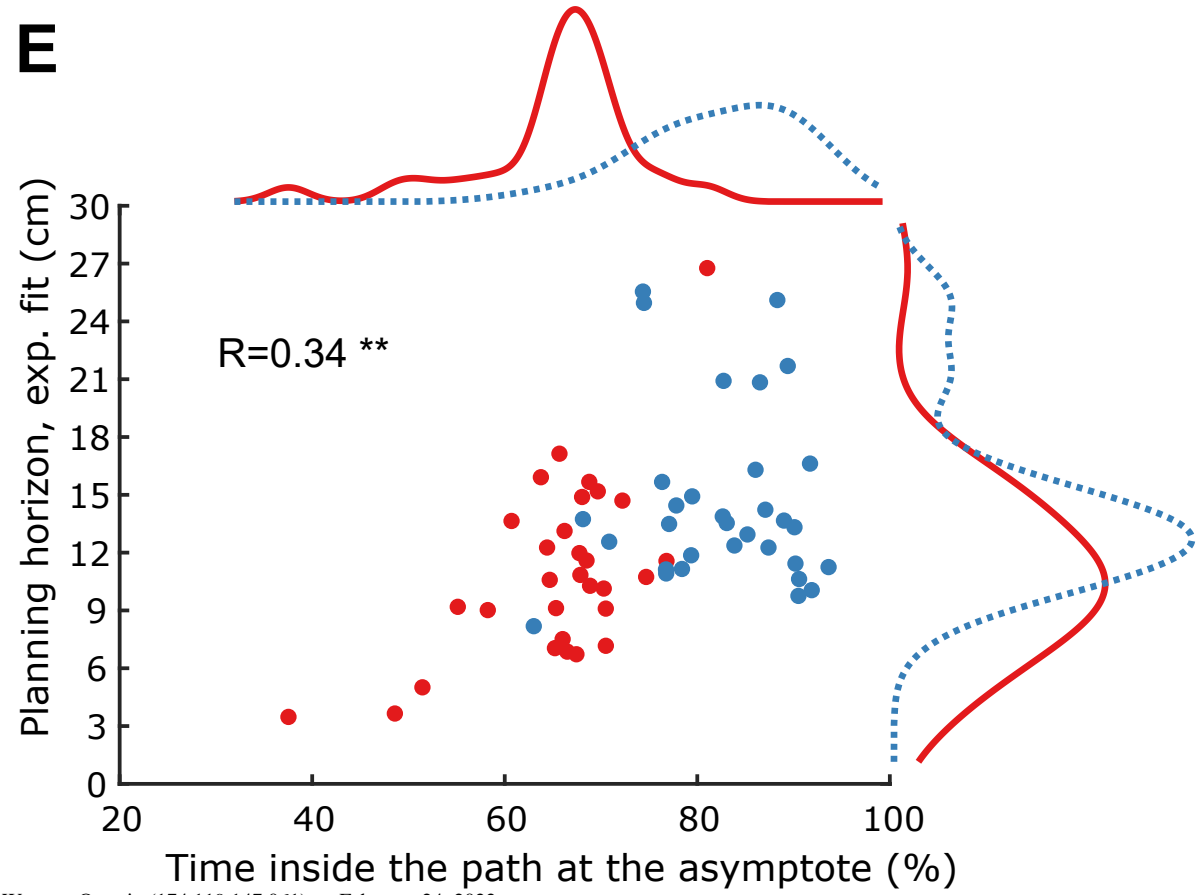
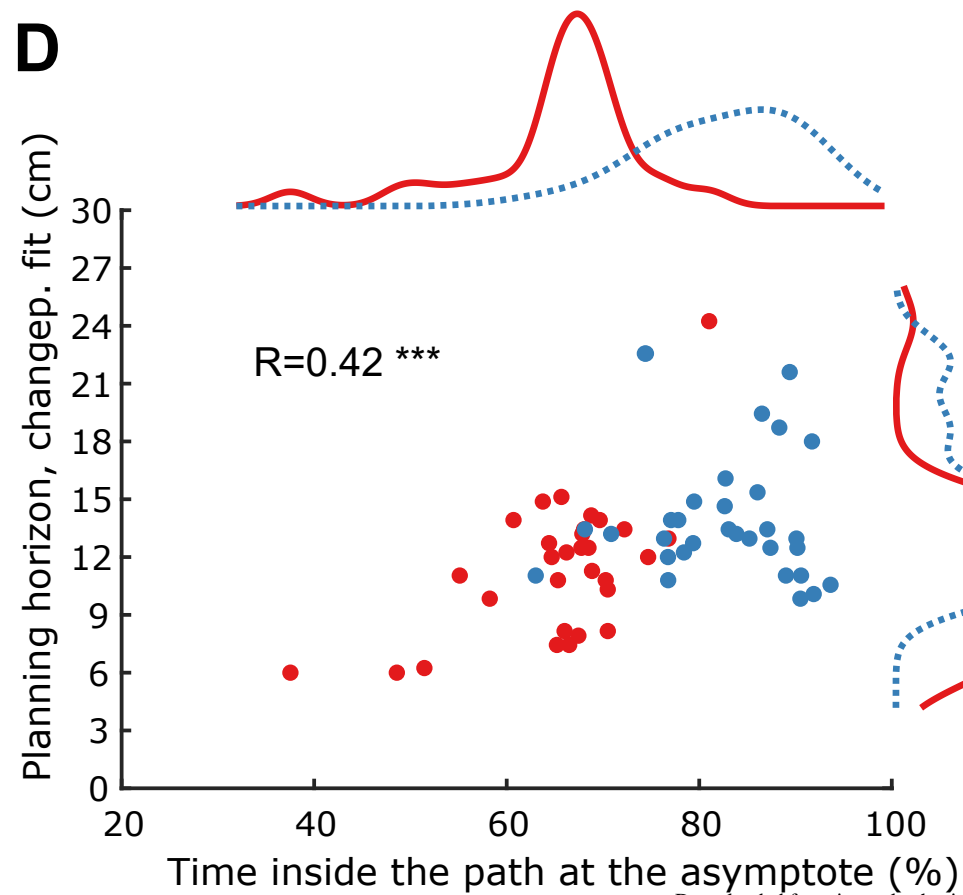
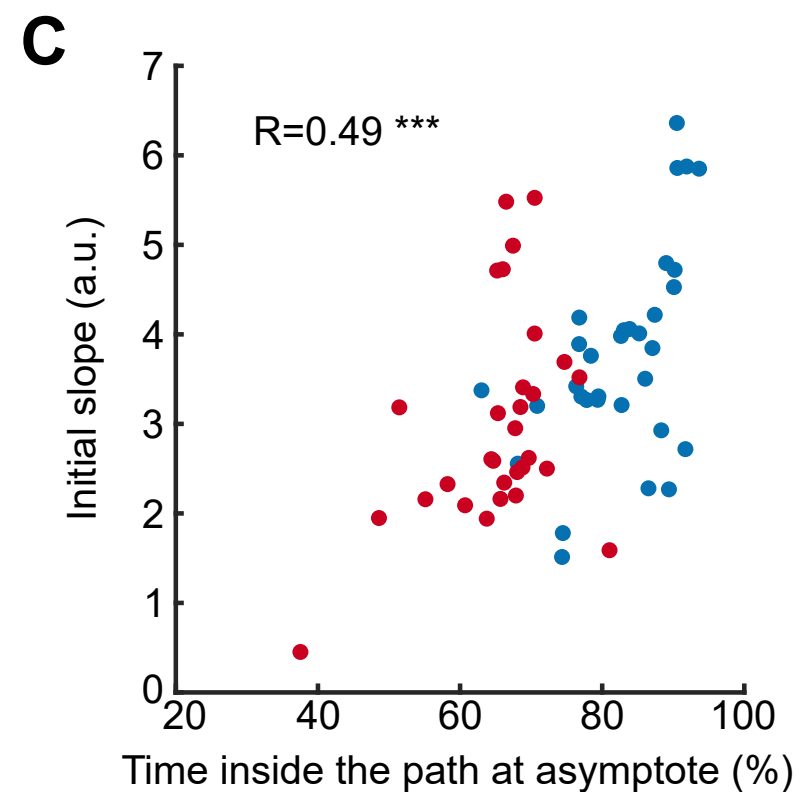
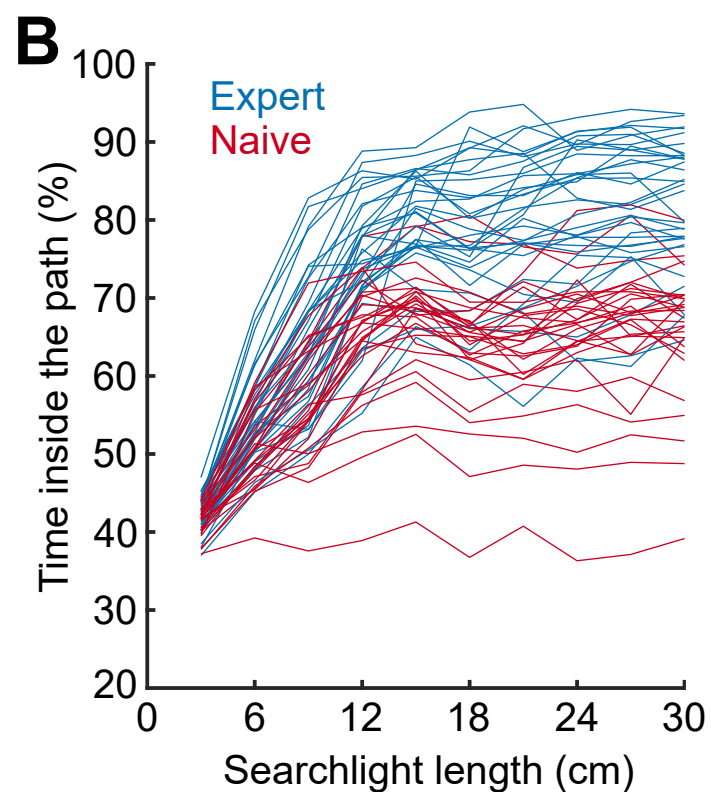
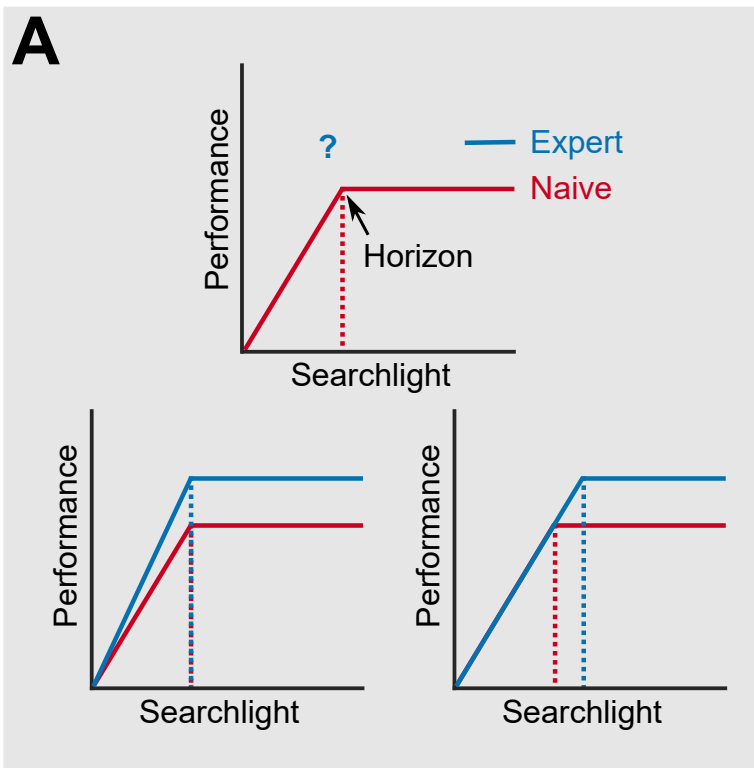
788 **Wolpert DM, Diedrichsen J, Flanagan JR.** Principles of sensorimotor learning. *Nat Rev*
789 *Neurosci* 12: 739–51, 2011.

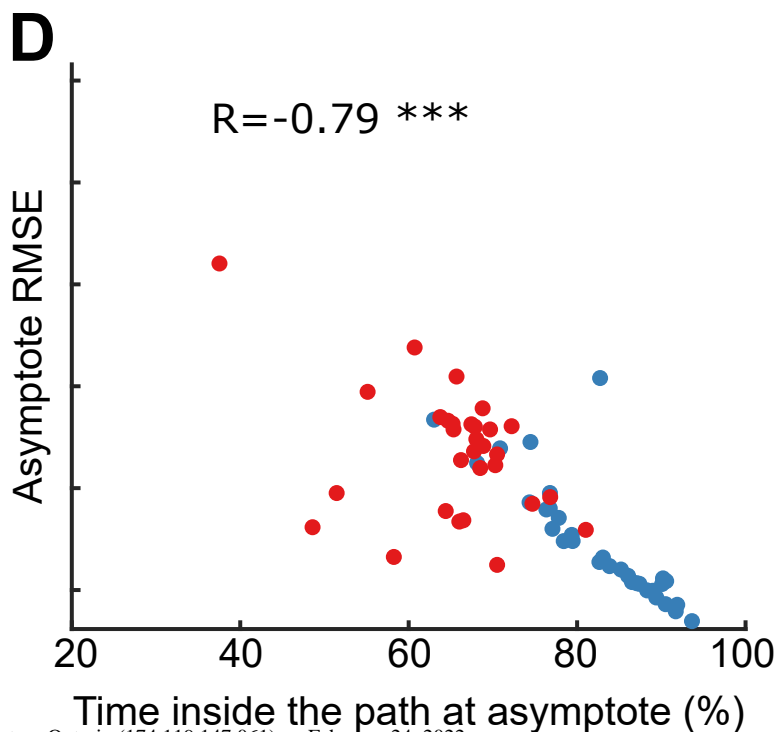
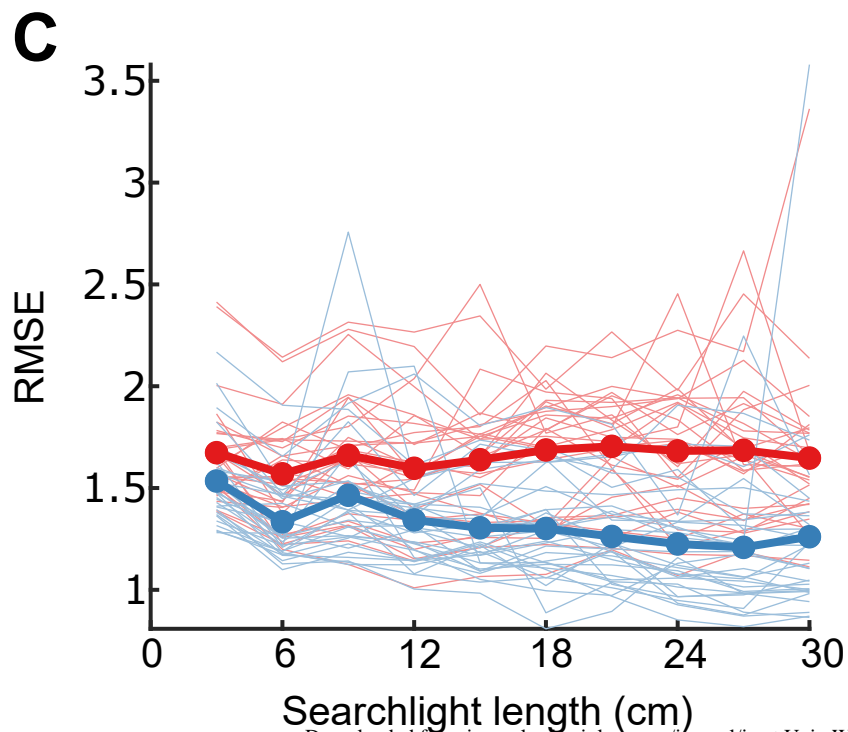
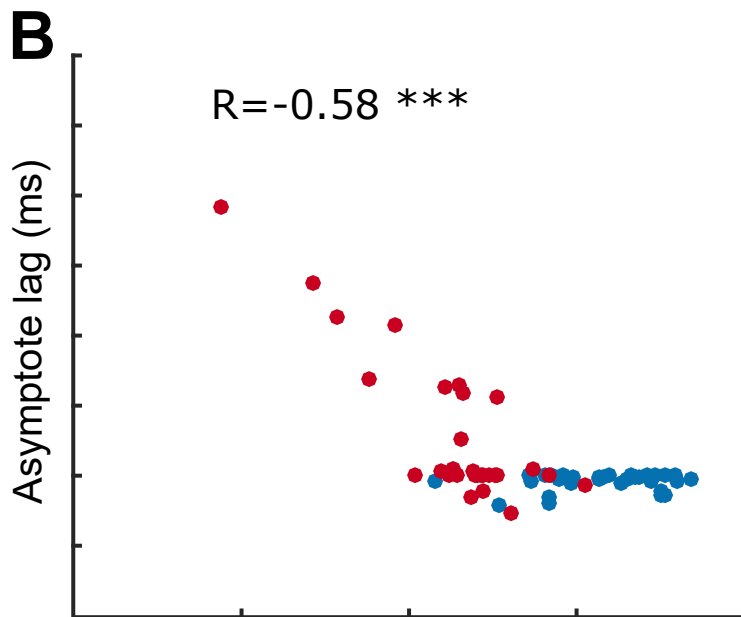
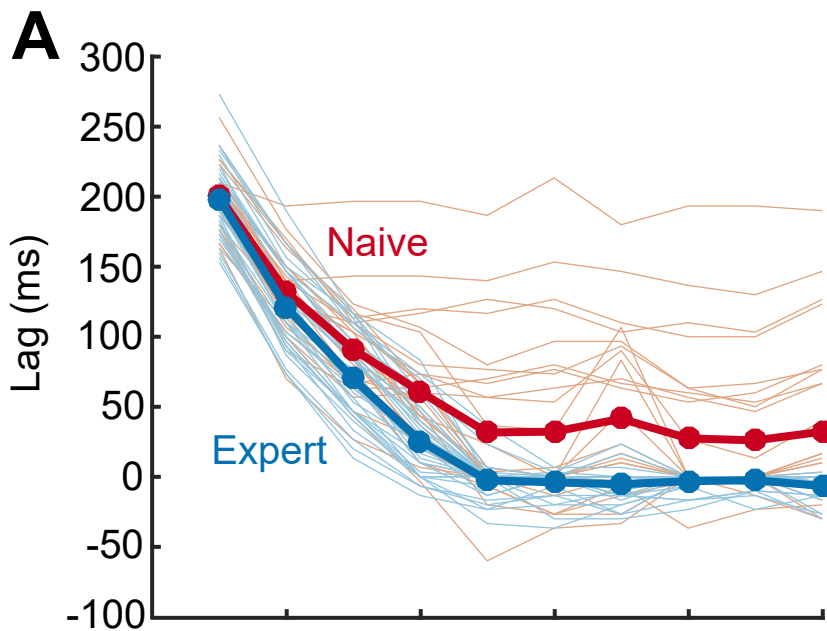
790 **Wong AL, Lindquist MA, Haith AM, Krakauer JW.** Explicit knowledge enhances motor
791 vigor and performance: motivation versus practice in sequence tasks. *J Neurophysiol*
792 114: 219–232, 2015.

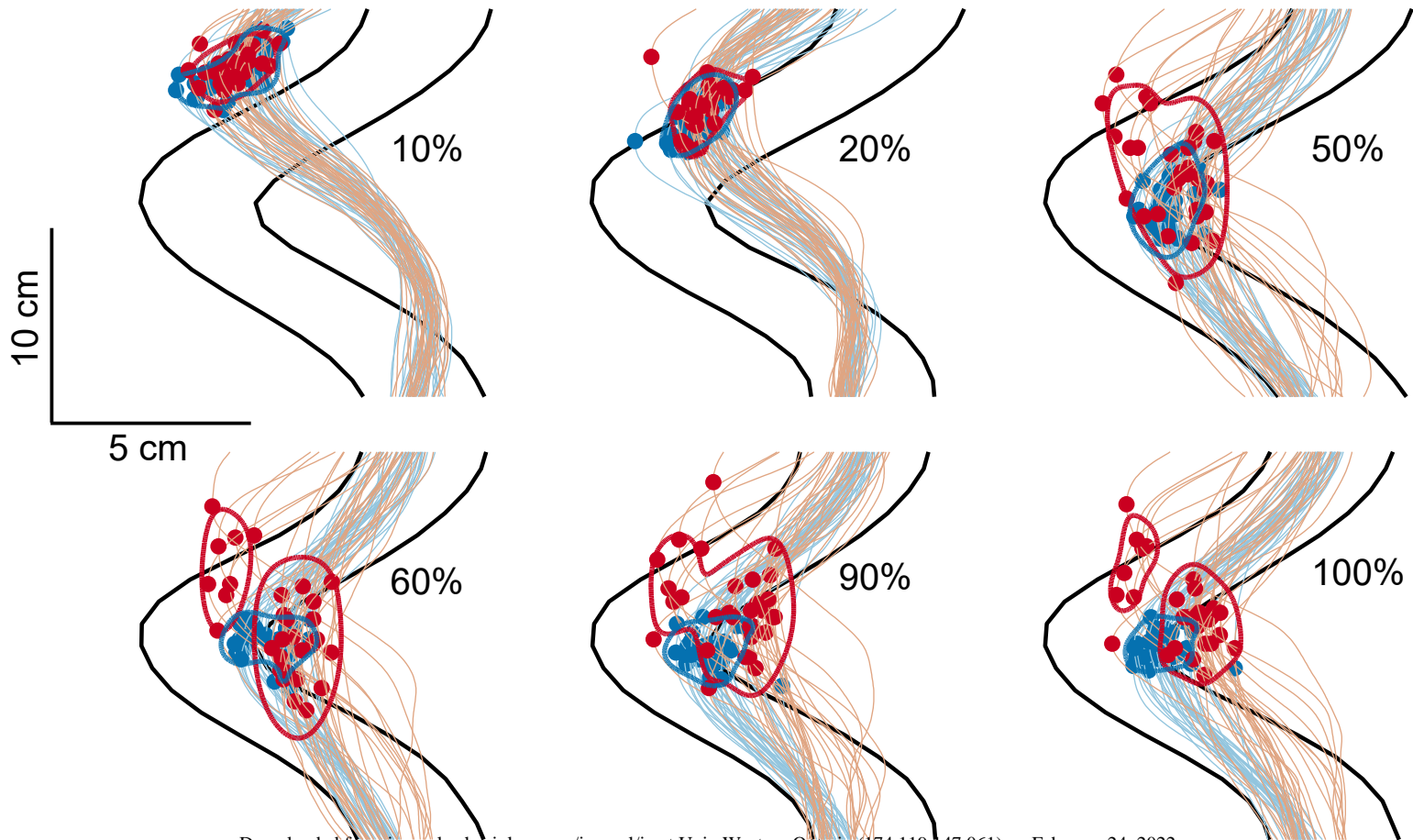
793

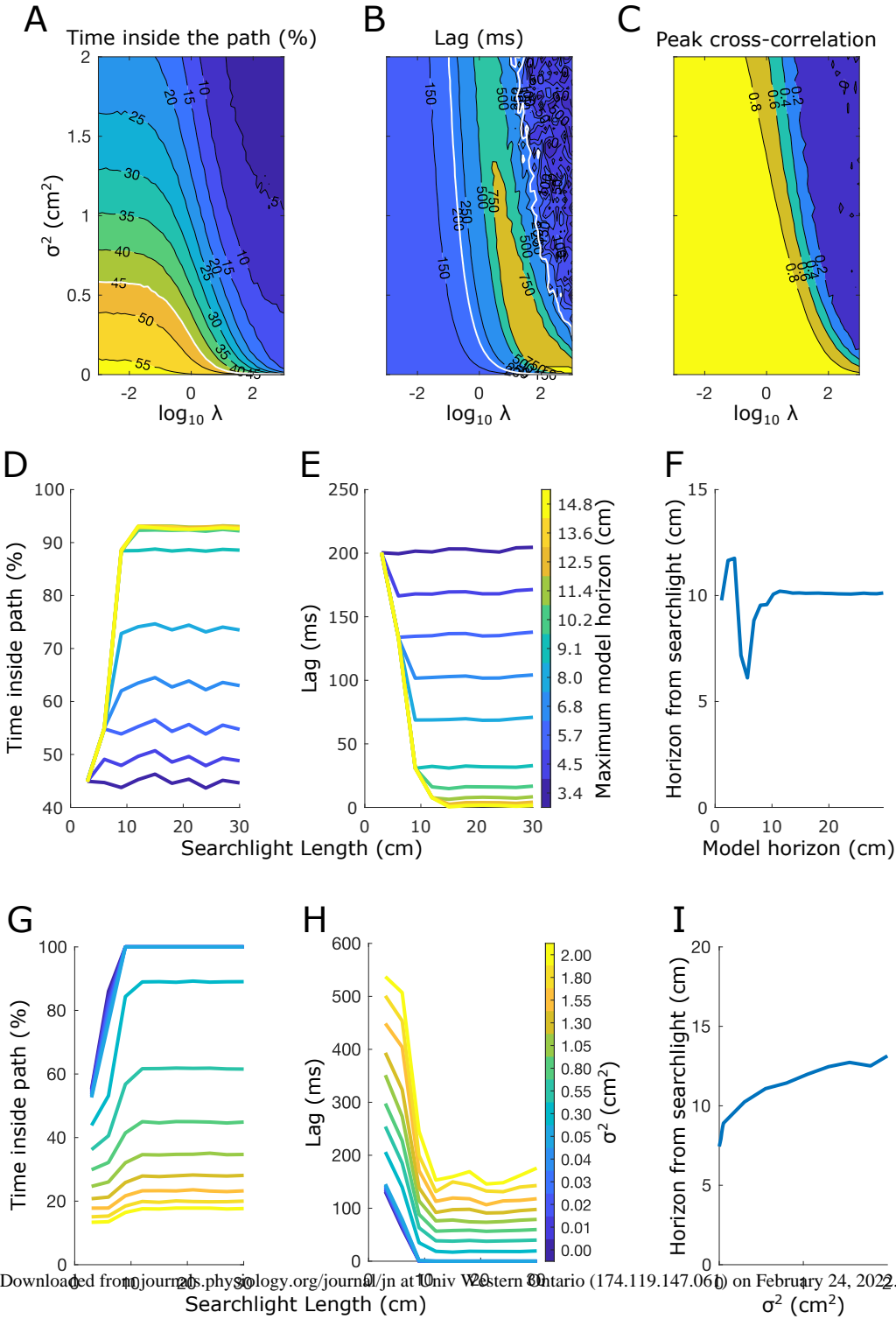
794

A**B****C**



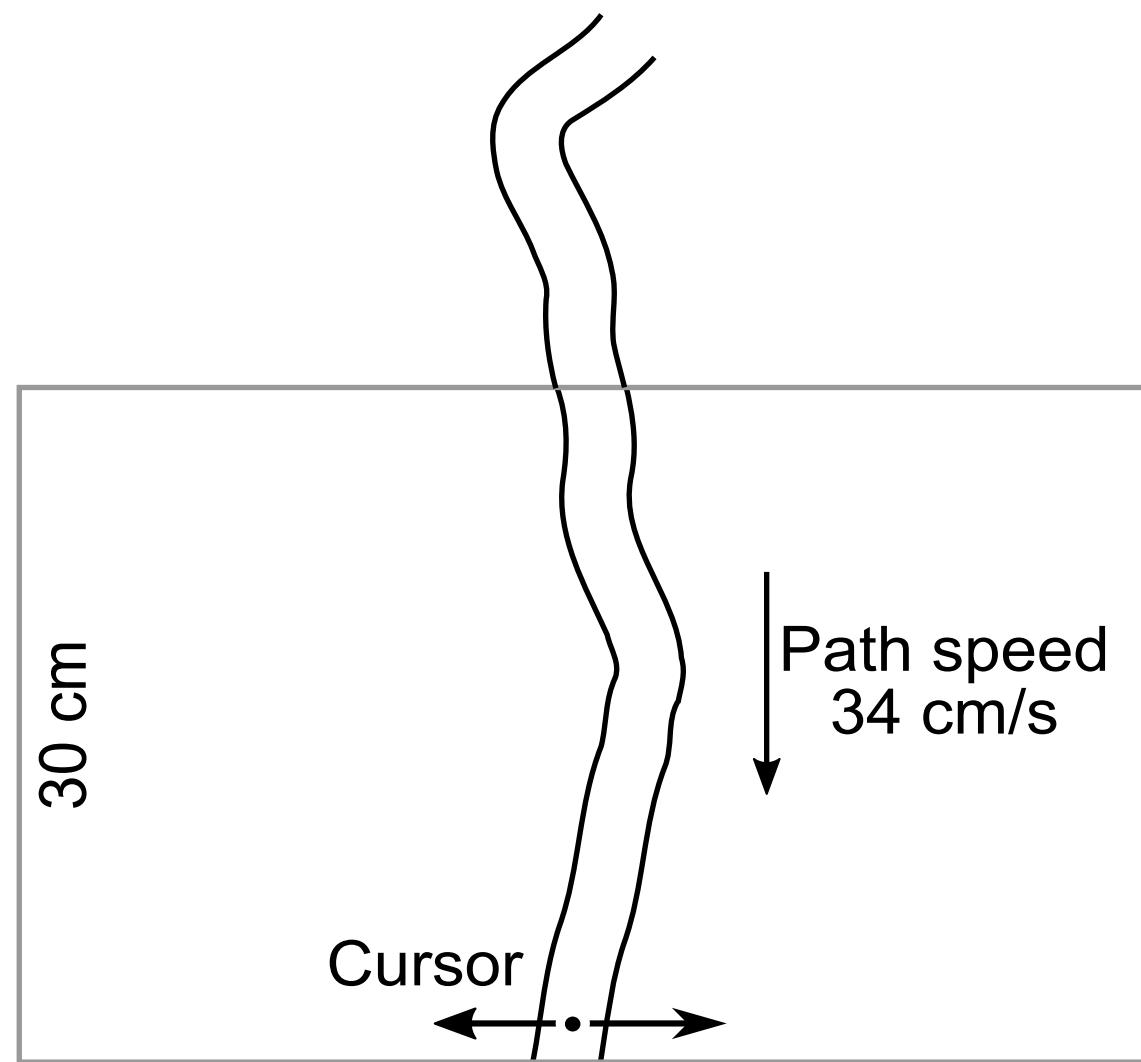




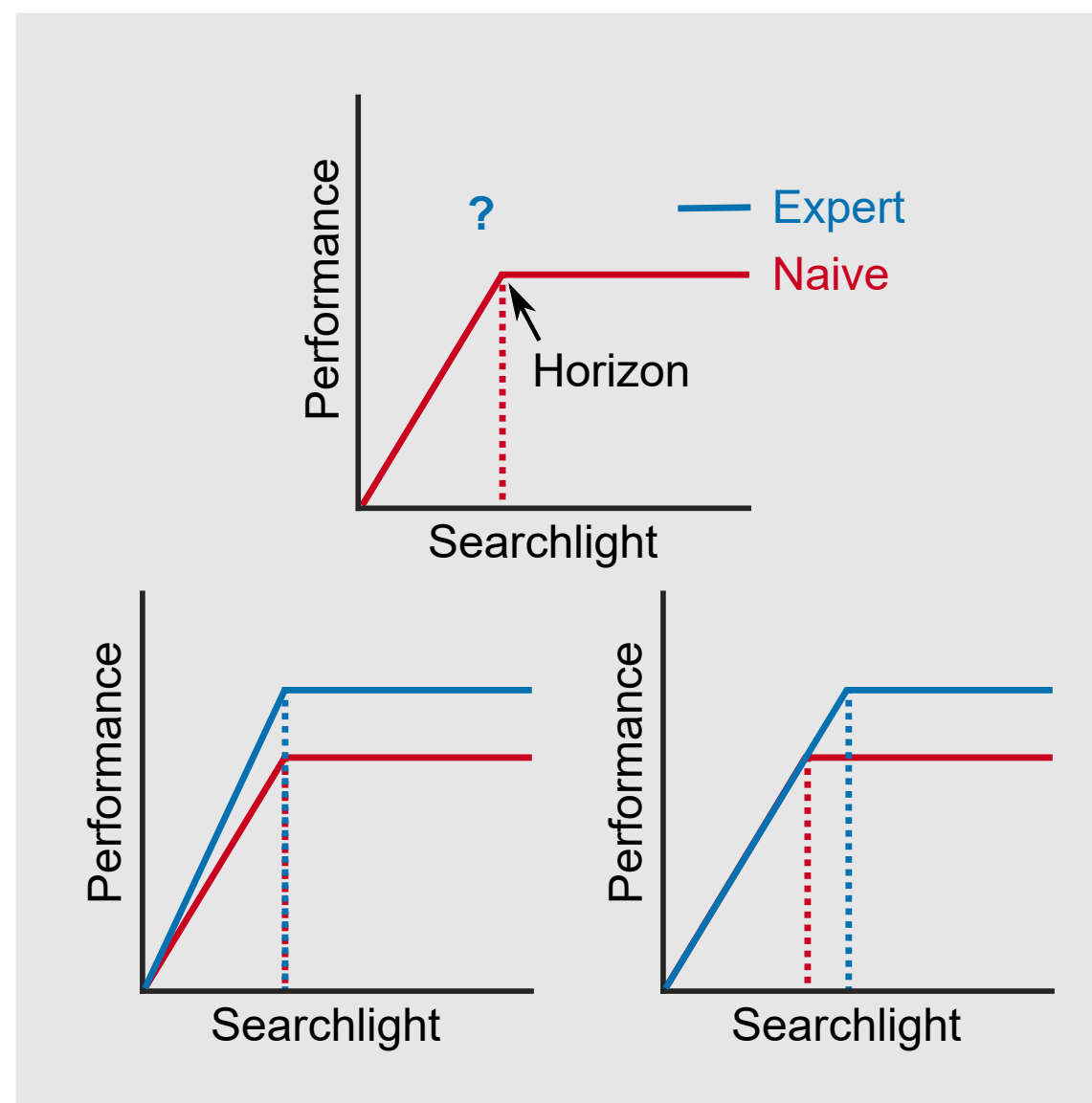
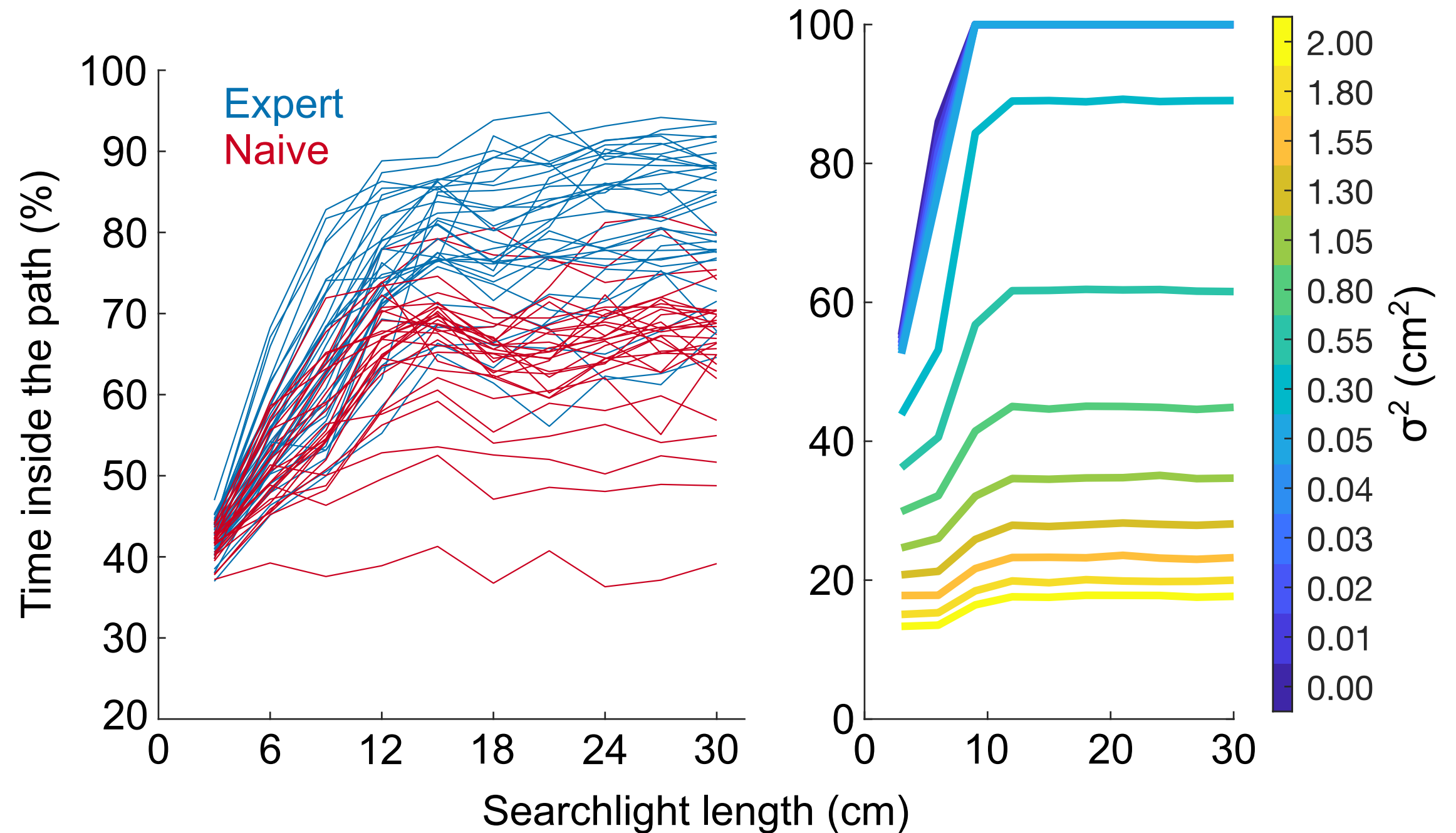


Motor skill learning decreases movement variability and increases planning horizon

Methods



Outcomes



Conclusion

Experts had a lower movement variability and took a longer section of the future path into account when performing the task. A receding horizon control model that increases with tracking still quantitatively captured the movement behavior.